Desalination and Water Treatment
www.deswater.com

doi: 10.5004/dwt.2021.27263

226 (2021) 408–418
June

Integration of water treatment sludge and agriculture waste as low-cost adsorbent for Remazol red dye removal

Sofiah Hamzah[a,b,*], Ng Boon Swan[b], Nurul Ashraf Razali[b], Nurul Aqilah Mohamad[a,b], Nazaitulshila Rasit[a,b], Asmadi Ali[a,b], Mohd Sofiyan Sulaiman[b], Ahmad Jusoh[b], Nur Hanis Hayati Hairom[c], Nora'aini Ali[b,d], Norhafiza Ilyana Yatim[d]

[a]*Environmental Sustainable Material Research Interest Group, Faculty of Ocean Engineering, Technology, and Informatics, Universiti Malaysia Terengganu, 21030 Kuala Nerus, Terengganu, Malaysia, Tel. 09-6683971; emails: sofiah@umt.edu.my (S. Hamzah), nurulaqilahmohamad@gmail.com (N.A. Mohamad), nazaitulshila@umt.edu.my (N. Rasit), asmadi@umt.edu.my (A. Ali)*
[b]*Faculty of Ocean Engineering, Technology, and Informatics, Universiti Malaysia Terengganu, 21030 Kuala Nerus, Terengganu, Malaysia, emails: ng.boon.swan@gmail.com (N.B. Swan), nrazali@umt.edu.my (N.A. Razali), sofiyan@umt.edu.my (M.S. Sulaiman), ahmadj@umt.edu.my (A. Jusoh), noraini@umt.edu.my (N. Ali)*
[c]*Department of Chemical Engineering Technology, Faculty of Engineering Technology, Universiti Tun Hussein Onn Malaysia, Hab Pendidikan Tinggi Pagoh, KM1, Jalan Panchor, 84600 Panchor, Muar, Johor, Malaysia, email: nhanis@uthm.edu.my*
[d]*Higher Institution Centre of Excellence (HICoE), Institute of Tropical Aquaculture and Fisheries, Universiti Malaysia Terengganu, 21030 Kuala Nerus, Terengganu, Malaysia, email: hafiza.ilyana@umt.edu.my*

Received 22 October 2019; Accepted 19 March 2021

ABSTRACT

This study aims to investigate the potential of integrating water treatment sludge and rice husk (RH) as a low-cost adsorbent for Remazol red (RR) dye removal. In the first stage of the study, a comparison was made for thermally-treated conventional water treatment sludge and desalination water treatment sludge (DWTS) in terms of the characteristics and potential of the adsorbents in removing RR dye. DWTS seemed to be a better adsorbent and was selected to be integrated with RH for better properties and performance. The RH was treated with sodium hydroxide solution. The integrated adsorbent (RH-DWTS) was characterised using scanning electron microscopy, Fourier transform infrared, and X-ray diffraction. The performance of the adsorbents to remove RR dye was evaluated by carrying out batch adsorption experiments at different adsorbent dosages, initial dye concentrations, and pH. The highest removal rate of RR (81.2%) was achieved through adsorption using RH5%-DWTS at 1 g/L adsorbent dosage, 30 mg/L initial dye concentration, and pH 3. The adsorption study fitted well the Freundlich isotherm model, indicating heterogeneous adsorption. The results of this study can provide an essential pathway for developing sustainable and cost-effective dye wastewater treatment in the future.

Keywords: Adsorbent; Rice husk; Sludge; Dye removal; Adsorption

* Corresponding author.

1. Introduction

The demand for clean water supply is growing in line with population growth and the economic sector's development. In Malaysia, the water production and consumption recorded in 2019 were 17,763 million L/d (MLD) and 11,540 MLD, respectively. Water consumption for the domestic category (household) accounted for 59.1% compared to 40.9% for the non-domestic (industrial) category. Three states recorded the highest water consumption: Selangor (30.1%), Johor (12.4%), and Perak (8.3%) [1]. Water pollution by the dye industry in Malaysia is not as critical as in other developing countries, but the growth of the textile industry due to consumer needs can contribute to severe pollution problems of water sources [2]. The most extensive textile industry in Malaysia is in Kelantan and Terengganu, with about 320 registered 'batik' factories. The wastewater discharged from 'batik' manufacturing is the primary source of water pollution in Kelantan due to lack of pre-treatment before discharge to water bodies [3].

About 2 million wastes are produced yearly worldwide to meet industry demands, such as plastics, food, paper, fabrics, cosmetics, medicines, inks, and paints [4]. The high demand for dyes in the textile industry has produced more than 8,000 chemicals in dyeing and printing processes. Dyes are naturally plant-based materials. However, synthetic dyes used in the fabric industry require many dyes. The textile industry is the largest user of dyes. More than 10,000 types of dyes and about 7×10^5 tonnes of dyes are produced annually due to the increasing demand from industries and consumers [5]. About 80% of the dye used will remain in the fabric, and the rest will be removed as the waste material in water. Continuous discharge and accumulation in water bodies for a long time result in high chemical oxygen demand and turbidity, and increase the total suspended solids. The characteristics of an intense coloured dye are a high degree of aromaticity and low biodegradability due to high molecular weight components, which can endanger aquatic organisms [6]. This phenomenon can cause the inhibition of UV light penetration through water, decrease the dissolved oxygen, and affect the photosynthetic activity of aquatic plants [7,8].

Dye molecules are chemical compounds that interact on fabric surfaces with the functional groups to impart colour and withstand detergent action [9]. The most widely used group is azo dyes, approximately 60%–70% with one or more azo groups (–N=N) attached to aromatic systems. Azo dyes can cause water pollution in the textile industry if these pollutants are not treated appropriately. The chromophore structure of azo dyes can chemically change through reduction, oxidation, acetylation, and chlorination reactions. Compounds that are more mutagenic and relatively more harmful to the environment can also be produced from the dyes [10]. Remazol red (RR) dye is an example of azo dyes that have been used in the textile industry due to its low cost and easy to give bright colours [11]. Remazol dyes have phytotoxicity, carcinogenicity, genotoxicity, and teratogenicity effects on frog embryos and are toxic to enzyme degradation metabolites [12].

Several treatment technologies for treating wastewater from the textile industry include physical and chemical treatment methods, such as adsorption, flocculation, coagulation, chemical oxidation, membrane separation, and biodegradation [13]. Some of these methods have significant drawbacks, such as high cost, low efficiency, and generate extra wastes. Ozonation treatment method does not completely break down dyes, requires high costs due to the short half-life (20 min), and demands continuous supply [14]. Electrocoagulation can remove dyes via precipitation or floatation but produces a large volume of sludge [15].

Adsorption is also an essential technology to treat dye wastewater. Adsorption is the adhesion of ions or molecules from a gas, liquid, or dissolved solid to surfaces [16]. The method is effective in treating industrial effluent. It is used in dye removal and effectively removes dissolved pollutants, such as organic or inorganic substances. In general, activated carbon is used to treat dye wastewater. It has a high adsorption efficiency but costly, especially for large-scale treatment. Furthermore, the efficiency of dye removal depends on the type of dyes.

Low-cost adsorbents for wastewater treatment have attracted much attention, and many researchers have studied the feasibility of using low-cost materials to produce adsorbents, such as copra, coffee husks, fruit wastes, seeds, and rice husk (RH). RH is a by-product of rice production, whereas water treatment sludge is the residue that accumulates in water treatment plants, and both materials are promising adsorbents that can remove dyes efficiently due to their low cost and high adsorption capacity. The chemical composition of RH consists primarily of cellulose (35%), followed by lignin (31%), hemicellulose (21%), soluble material (4%), and moisture (1.1%) [17]. The high content of carbon (C) and silica (Si) in RH makes it very suitable to be used as an adsorbent of contaminants present in water [18]. RH has demonstrated good potential after modification by isolating certain compounds, such as Si [19,20], C [21], or cellulose [22,23]. Furthermore, dye adsorption capacity has been improved by adding other compounds, such as alginate [24], Ag/AgBr nanoparticles [25], and many more.

Wastewater treatment sludge (WTS) is a typical by-product formed from clean water processing using aluminium or iron-based salts as a coagulant. Aluminium salts (e.g., $Al_2(SO_4)_3 \cdot 18H_2O$), ferric ion salts (e.g., $FeCl_3 \cdot 6H_2O$), and ferrous iron salts (e.g., $FeCl_2$, $FeSO_4 \cdot 7H_2O$) are among commonly used coagulants. Sludge also includes organic compounds, suspended matter, and microorganisms. Sludge contains different oxides (e.g., CaO, MgO, Na_2O, K_2O, P_2O_5, and TiO_2) in small concentrations with SiO_2 as the main composition, and the composition also depends on the source of raw water [26]. Previous studies reported that the reuse of WTS as a coagulant associated with adsorbents could improve pollutant removal capacities, such as particulates, arsenate, boron, phosphorous, and heavy metals [27].

Therefore, this study aims to enhance the performance of RH as an adsorbent for RR removal by integrating with WTS. Two potential WTSs were utilised for comparison purposes: conventional water treatment sludge (CWTS) and desalination water treatment sludge (DWTS). Different sources of raw water produce different physicochemical properties of sludge. Therefore, the morphology, functional groups, and crystalline structure of RH, CWTS, and

DWTS were characterised using scanning electron microscopy (SEM), attenuated total reflection-Fourier transform infrared (ATR-FTIR), and X-ray diffraction (XRD). The performance of the adsorbents for different formulations of RH/WTS based on contact time, adsorbent dosages, pH, and different initial concentrations was evaluated.

2. Methodology

2.1. Materials

RH was collected from a rice mill in Besut, whereas CWTS was obtained from Kepong 2 water treatment plant in Kuala Terengganu, and DWTS was collected from a desalination water treatment plant in Bachok, Kelantan. Meanwhile, the dye wastewater was obtained from a 'batik' factory in Kelantan. Sodium hydroxide (NaOH) and hydrochloric acid (HCl) were purchased from Honeywell Fluka™ and were not of analytical grade.

2.2. Preparation of adsorbents from RH and WTS

RH was cleaned with distilled water and dried at 110°C for 12 h and sieved. Then, RH with an average particle size of 1.0 mm was collected and calcined at 400°C for 90 min. NaOH solution with a weight ratio of 1:3 was used to treat the RH. The RH treated with NaOH was dried at 120°C for 12 h and then calcined at 400°C for 20 min. The furnace temperature was increased from 400°C to 800°C and kept constant for 60 min to treat the RH. Finally, the pre-treated RH was ground and sieved. The treated RH was neutralised using 0.1 M HCl solution and washed several times with distilled water until the pH was constant (6.6–7.0). The washed and treated RH was then dried under vacuum at 120°C for 24 h. The WTS was dried at 110°C for 24 h in a laboratory oven and crushed into a particle size of less than 0.1 mm. The performance of RH, DWTS, and CWTS was evaluated by batch adsorption experiments for RR dye removal.

To integrate the RH and WTS, 5 wt.% of treated RH was mixed well with DWTS and distilled water to ensure the mixture homogeneity. The mixture was dried at 95°C for 24 h and placed in a furnace for 3 h at 900°C, and then denoted as RH5%-DWTS.

2.3. Characterisation of adsorbents

A scanning electron microscope (JSM P/N HP475 model) was used to study the adsorbent morphology. The samples were coated with a thin gold layer to improve the imaging of the RH samples. The surface functionalities of the adsorbents were determined using FTIR and recorded in the range of 4,000–400 cm^{-1}. The crystalline structure of the adsorbents was identified through XRD using 18 kW Cu-Kα radiation. The voltage and intensity applied were 45 kV and 40 mA, respectively. The diffraction angle (2θ) was varied from 0° to 80° to identify any crystal morphology changes and intermolecular distances between the polymer's inter-segmental chains, and the counting time was 1 s at each angle step [28]. All adsorbents were ground into powder form prior to characterisation.

2.4. Batch adsorption experiments

Batch adsorption tests were performed to determine the best conditions for the adsorption of RR onto the adsorbents, including (i) the effect of type of adsorbents, (ii) the effect of adsorbent dosage, (iii) the effect of initial concentration, and (iv) the effect of pH.

For the first stage of the batch experiment, the prepared adsorbent with a fixed dosage of 1 g/L was mixed with 50 mL of RR dye solution (initial dye concentration of 30 mg/L at pH 3) in a conical flask and shaken at room temperature at 130 rpm for 15–180 min. The solution and residue were centrifuged at 3,000 rpm for 10 min (Model 5702 R). The suspension was filtered using Whatman filter No. 42 and the obtained filtrate was analysed using an ultraviolet-visible (UV-vis) spectrophotometer at 518 nm for the RR dye content. All experiments were repeated three times. The mentioned techniques were also used for adsorption studies at different adsorbent dosages (1–4 g/L), initial dye concentrations (5–30 mg/L), and initial pH values (3–11). The NaOH solution (0.1 N) and nitric acid solution (0.1 N) were used for pH value adjustment. The efficiency of adsorption capacity was calculated using Eq. (1):

$$q_e = \frac{\left(C_0 - C_e\right)}{W} V \tag{1}$$

where C_0 and C_e (mg/L) are the initial RR dye concentration and equilibrium concentration of dye solution, respectively, V (L) is the volume of dye solution, and W (g) is the mass of adsorbent.

2.5. Adsorption isotherm

Langmuir and Freundlich's models were used to correlate the experimental equilibrium adsorption data of dye adsorption with the integrated adsorbent (RH5%-DWTS). The Langmuir equation [29] is expressed in Eq. (2):

$$\frac{C_e}{q_e} = \frac{1}{Q_m b} + \frac{C_e}{Q_m} \tag{2}$$

where Q_m is the monolayer adsorption capacity (mg/g) and b is the Langmuir isotherm constant related to the binding sites' affinity and adsorption energy (L/mg).

The Langmuir equation assumes that the maximum adsorption of an adsorbate matches a monolayer formation by the adsorbate molecules or ions on the adsorbent surface, which is homogeneous. Also, the Langmuir isotherm forecasts that the intermolecular forces decrease rapidly with the distance. The existence of a monolayer of adsorbate at the adsorbent's outer surface is consequently predicted by the model. The Langmuir model better fits monolayer adsorption on the adsorption sites with uniform energy. It is more applicable at low concentration ranges as compared to the Freundlich model.

The Freundlich isotherm [29] is presented in Eq. (3):

$$\log q_e = \log K_f + \frac{1}{n} \log C_e \tag{3}$$

where q_e is the amount of dye adsorbed (mg/g), C_e is the equilibrium concentration of dye in solution (mg/L), and K_f and n are the constants incorporating the adsorption capacity and adsorption intensity, respectively.

The Freundlich isotherm model is an empirical equation that accomplishes the heterogeneity of the surface. It is based on the exponential distribution of active sites and their energies. The Freundlich model is better in simulating the adsorption on a heterogeneous adsorbent surface, where the lower value of $1/n$ will produce high heterogeneity of the adsorbent's surface [30]. The model is more applicable for adsorption at high concentration ranges [31]. The graph of $\log q_e$ vs. $\log C_e$ will give a straight line with a slope of $1/n$ and an intercept of $\log K_f$.

2.6. Statistical analysis

Isotherm model equations can be used to visualise the effect of experimental factors on adsorption. Statistical data analysis is a crucial procedure for performing various statistical operations. In this research, analysis of variance (ANOVA) and the sum square error (SSE) of prediction were used to analyse the data obtained.

ANOVA is a statistical tool that segments the total variation in a set of data into parts associated with specific variation sources for testing hypotheses on the model's parameters. The null hypothesis for an ANOVA is that there is no significant difference among the selected groups, while the alternative hypothesis assumes that there is at least one or more significant difference among the selected groups. *F*-values represent the most variation in response that can be explained by the empirical model. When the *p*-value associated with the *F*-value is smaller than 0.05, then the null hypothesis is rejected. In other words, the alternative hypothesis is supported. If the null hypothesis is rejected, it can be concluded that the means of all the groups are unequal. In this research, ANOVA was used to interpret the significance of the adsorbent's performance.

The SSE is the sum of the squared differences between each observation and its group means. In general, it can be used as a measure of variation within a group. If all cases within a group are identical, then the SSE will be equal to 0. The fit will be more useful for prediction when the SSE value is closer to 0, indicating that the model has a minor random error component.

3. Results and discussion

3.1. Characterisation of adsorbents from CWTS and DWTS

The morphology of the adsorbents was characterised using SEM and FTIR. SEM is a useful and powerful magnification tool for observing and examining the surface structure and morphology of a material and identifying its chemical composition. Fig. 1 shows the SEM images of CWTS and DWTS. From the micrographs obtained (Fig. 1a), the surface texture and pore development of the adsorbents are visible and exhibit a rough surface where large quantities of agglomerates are distributed. The dried flocs of DWTS in Fig. 1b are flakier and largely fragmented [32]. The surface image of the sludge is also affected by the composition of chemical compounds that exist on the surface. The presence of aluminium, sulphur, calcium, and silicon can also produce needle-shaped crystals and cubic-shaped sludge surfaces [33]. Different salinity concentrations of water sources suggest different frameworks of dried sludge produced.

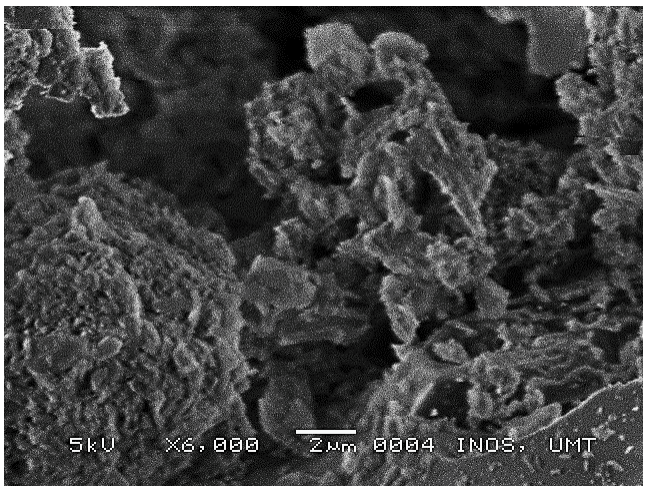

(a)

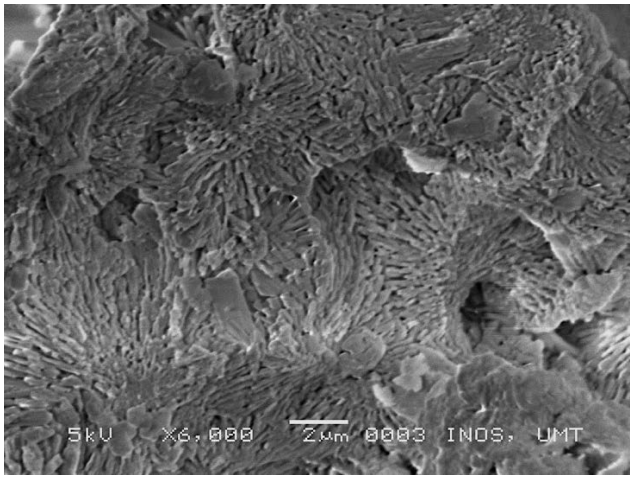

(b)

Fig. 1. SEM micrographs of (a) CWTS and (b) DWTS.

The surface functional groups determined from the FTIR analysis predominantly influenced the adsorption characteristics of the adsorbents. The FTIR analysis spectrum provides information about the molecular structure of the functional groups present on the samples. A complicated spectrum usually gives more adsorption bands than a simple spectrum with few IR active covalent bonds. The FTIR spectra of CWTS and DWTS are shown in Figs. 2a and b, respectively. A sharp band in the spectra of CWTS at 3,428 cm^{-1} represents the OH stretching group, whereas the band at 1,637 indicates the presence of the CO group [34], which can assist in the adsorption process [35]. For DWTS, the peak at 1,423 cm^{-1} represents the existence of C–C–H asymmetric stretching [34].

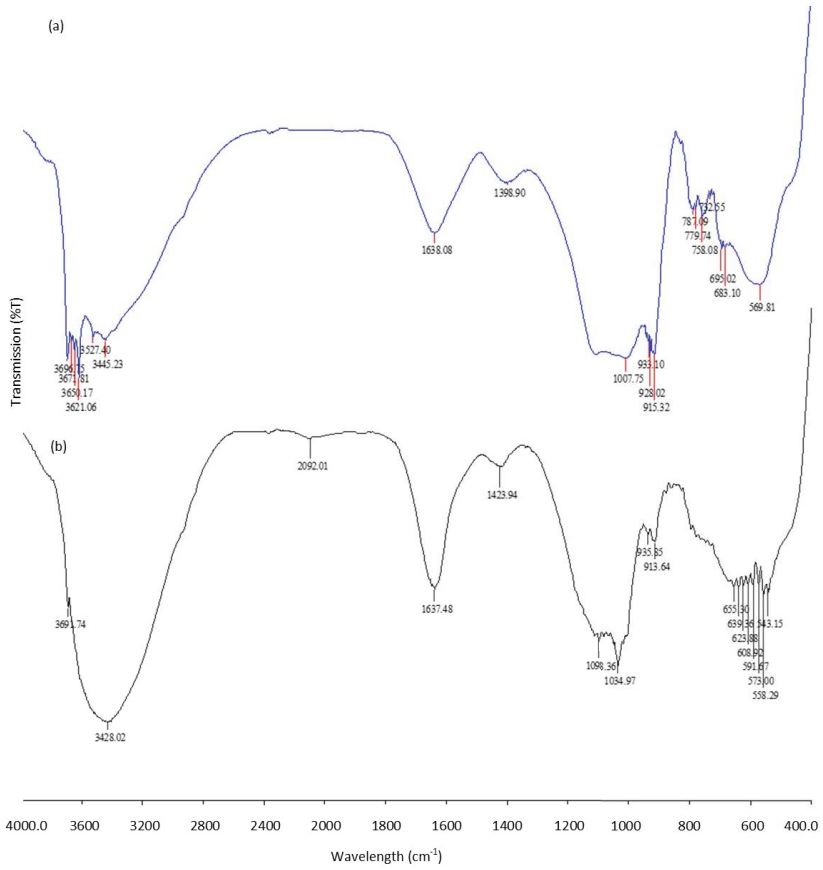

Fig. 2. FTIR spectra of (a) CWTS and (b) DWTS.

3.2. Performance evaluation of CWTS and DWTS for RR dye removal

A comparison was made for both adsorbents in RR dye removal in the early stage of the study, and the results are shown in Fig. 3. DWTS demonstrated better adsorption capacity as the adsorbent successfully removed 80.5% RR dye compared to CWTS, which could only remove 75% RR dye at the saturation time of around 90 min.

The finding shows that the presence of OH, CO, and C–C–H asymmetric stretching assists the adsorption of RR dye onto the adsorbent, which consequently improves the percentage removal. Therefore, DWTS was chosen to be integrated with RH for the subsequent experiments.

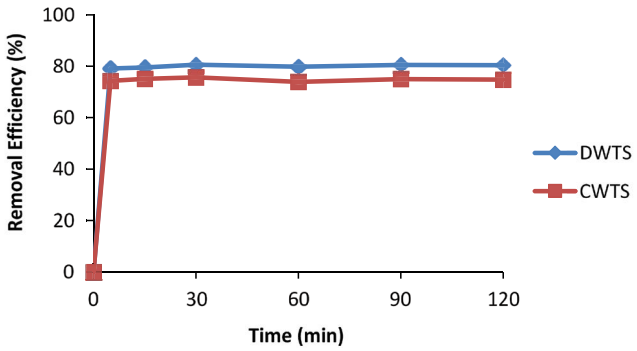

Fig. 3. The percentage removal of RR dye by CWTS and DWTS.

3.3. Characteristics of the integrated adsorbent RH-DWTS

Based on the SEM micrographs of the integrated adsorbent RH-DWTS in Fig. 4, RH was successfully deposited with DWTS. The irregular shapes of the flakes represent the successful deposition of DWTS, which coated the rough surface of RH.

The porosity of adsorbents can be increased by treating RH with an alkaline solution of NaOH to produce rough surfaces [36]. The modification of RH using WTS will increase adsorption capacity due to increased surface porosity. Besides, thermal treatment using high temperatures can also potentially increase the porosity of WTS [37]. Fig. 5a represents the FTIR spectra of RH-DWTS. The spectrum of RH-DWTS shows a broadband at around 3,447 cm^{-1}, indicating the hydrogen bonding interaction combined with available silanols and the presence of physisorbed water on the sludge surface.

The strong band at 1,097 cm^{-1} can be attributed to the stretching of Si–O–Si of silica, while the band around 1,637 cm^{-1} is considered the bending vibration of water molecules bound to the Si matrix. The increase of transmission intensity in Fig. 5b is also due to the presence of a peak at 1,098 cm^{-1} of DWTS, suggesting the increase of

the Si content of RH with the presence of the deposited DWTS. Both spectra display the O–H stretching vibration (3,400–4,000 cm^{-1}), indicating water, alcohol, and phenol compounds. The peak at 795 cm^{-1} shows that hydroxide groups are bound to one iron and one aluminium or magnesium neighbour [35].

The mineral composition of the adsorbents was identified through XRD analysis, and the results are shown in Fig. 6. The ignition of samples at high temperatures suppresses the interference of clay peaks with quartz, reduces the initial matrix variation of samples, and increases quartz peaks' relative intensity [35]. The narrow and sharp peaks shown in the graph indicate that the adsorbents possessed high crystallinity with high surface charge density, which enhanced the electrostatic attraction with the dye molecules.

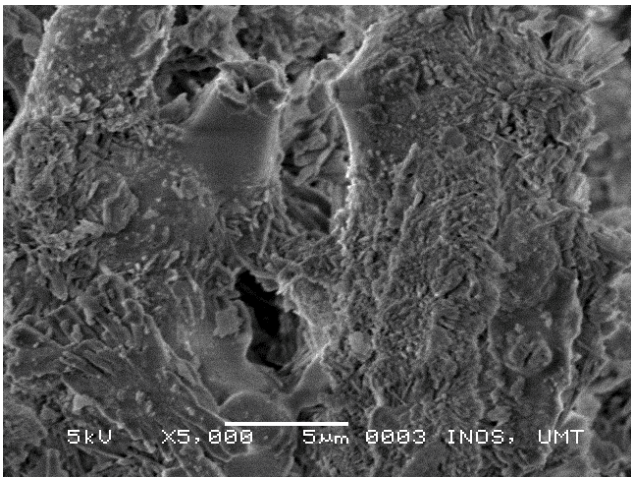

Fig. 4. SEM morphology of the integrated adsorbent RH-DWTS.

3.4. Performance of the integrated adsorbent RH-DWTS for RR dye removal

3.4.1. Effect of adsorbent dosage

Fig. 7 presents the percentages of RR dye removed at different adsorbent dosages. The adsorbent dosage of 1.0 g/L demonstrated the highest adsorption capacity, with 81.4% RR dye removed, while only 77% RR dye was removed upon introducing 4.0 g/L of RH5%-DWTS. The effect of adsorbent dosage for RR dye removal by RH5%-DWTS decreased with increasing adsorbent dosage. A possible explanation for this finding might be that the increase in the amount of adsorbent reduced the total surface area available for adsorption due to aggregation or overlapping of adsorption sites [38].

The time required for decolourisation increased from 0 to 5 min of contact time, showing rapid adsorption of RR dye on adsorbent's surface with different dye concentrations (1–4 g/L). The use of RH (10 g/L) as a supplement in Bushnell-Haas medium for *Galactomyces geotrichum* MTCC 1360 enhanced RR dye's decolourisation to 86% over 72 h at pH 11 [39]. Adsorption efficiency depends on a large number of active sites, high surface functionality, and a porous structure [40].

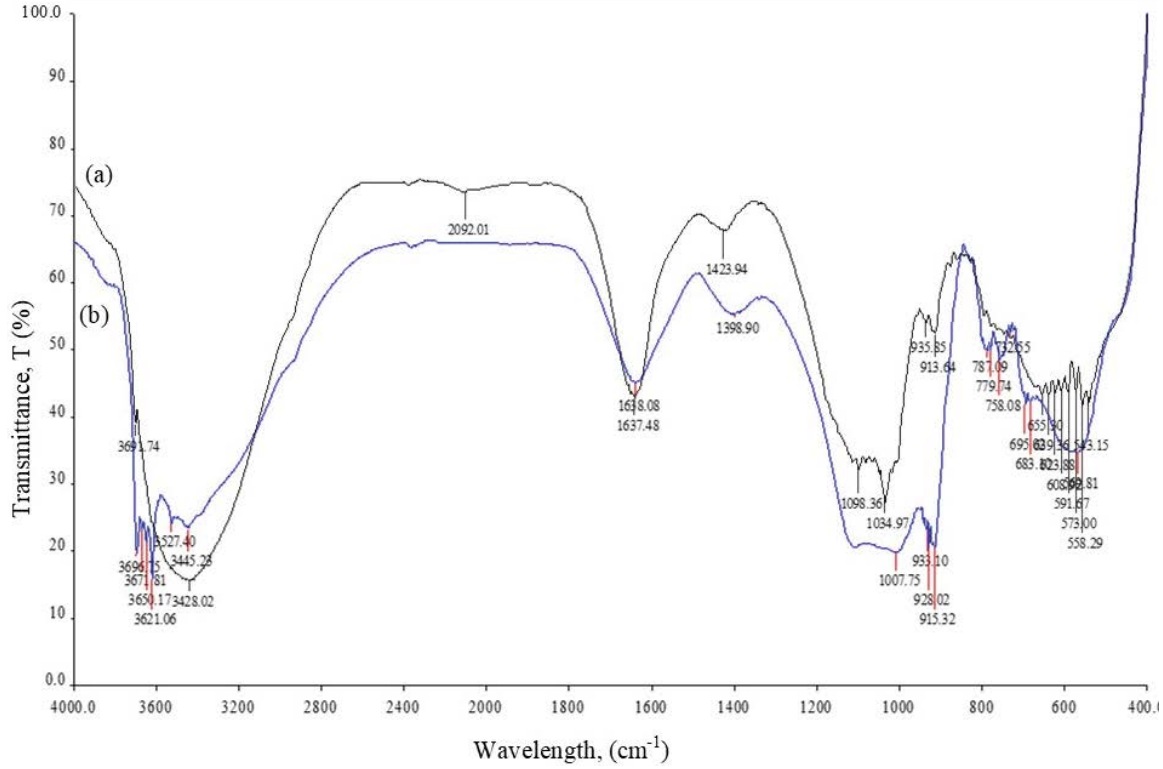

Fig. 5. FTIR spectra of (a) DWTS and (b) RH5%-DWTS.

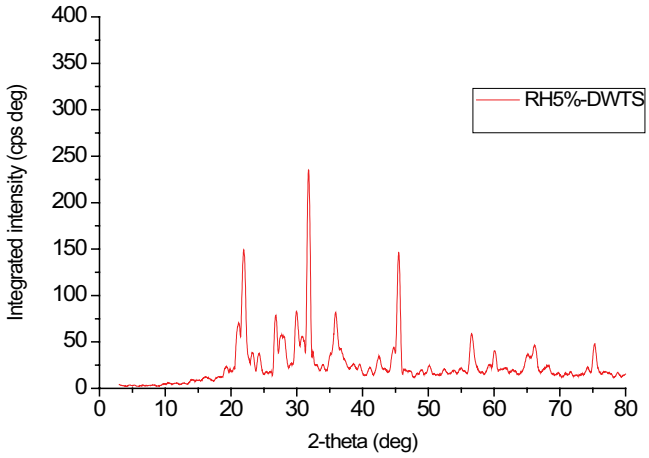

Fig. 6. XRD patterns of RH5%-DWTS.

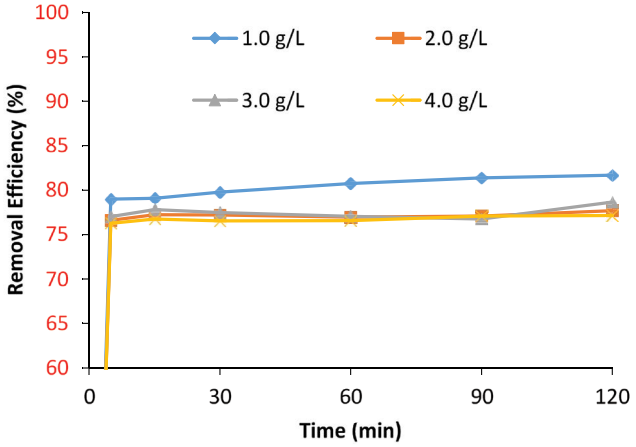

Fig. 7. The percentage removal of RR dye for different adsorbent dosages (adsorption condition: room temperature; initial dye concentration of 30 ppm; pH 3).

3.4.2. Effect of initial concentration

One of the most significant factors affecting the adsorption capacity of an adsorbent is the initial concentration of a solution. 50 mL of RR dye solutions ranging from 5 to 30 mg/L (pH 3) were prepared for the batch adsorption study using 1.0 g/L of the integrated adsorbent at room temperature with an agitation speed of 150 rpm. The obtained results are displayed in Fig. 8.

Fig. 8 shows two different regions of the adsorption in this study. The adsorption's initial stage is fast and rapid, and the second stage is relatively near the equilibrium. It is expected that the number of active adsorbent sites is higher during the initial stage, leading to better adsorption performance. However, the number of active sites decreased over time and becomes insufficient for the adsorption of dye molecules to occur [38].

Based on the figure, the initial concentration of 30 mg/L showed the highest percentage removal in this study, which is 81.4%. Meanwhile, the initial concentration of 5 mg/L showed the lowest percentage of removal, which

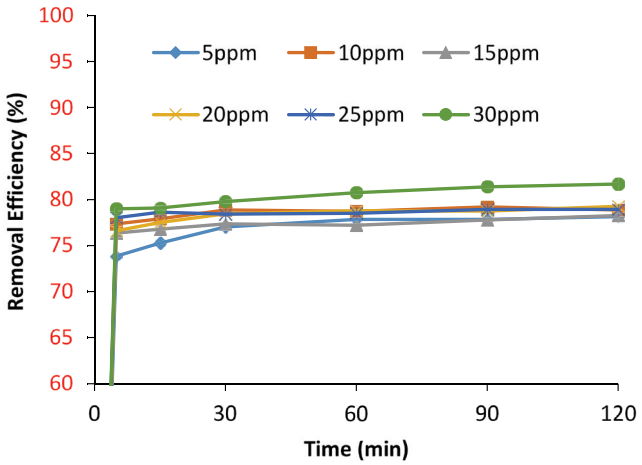

Fig. 8. The percentage removal of RR dye for different initial concentrations of dye solutions (adsorption condition: room temperature; adsorbent dosage of 1 g/L; pH 3).

is only 77%. The results indicated that the adsorption of dye molecules depends on the initial concentration of the solution. More ions or molecules are available in the dye solutions with higher initial concentrations than the dye solutions with low initial concentrations.

3.4.3. Effect of pH

Fig. 9 shows that the maximum removal of RR dye occurred at pH 3 (81.4%). A further increase in the pH value (pH 5 and pH 7) reduced the percentages of dye removal to 77.7% and 78.0%, respectively. Only 77.5% and 74.9% of dye removal occurred for alkaline dye solutions with pH 9 and pH 11, respectively. Therefore, the optimum pH 3 was selected for further studies in this research.

The adsorbent's maximum adsorption capacity can be affected by the pH of RR dye solution by modifying the ionisation of the binding groups, either by decreasing or increasing the competition between dye molecules and positively-charged species for active sites [41]. The pH values (pH 3–pH 11) are chosen by considering the electrostatic attraction between the adsorbent's positively-charged surface, mainly due to the anionic dye (e.g., RR dye).

In this case, the adsorption capacity decreased by increasing the pH value of the aqueous solution. A dye solution with a low pH value has higher H^+ ions, thus increasing the number of positively-charged adsorbent active sites and promoting adsorption. Positively-charged active sites probably favoured the adsorption of a negatively-charged dye, such as RR dye. The functional groups of RH waste, such as hydroxyl, carboxylic, and amide, are involved in the adsorption of dyes [41]. Furthermore, electrostatic attraction increases with decreasing pH, thus increasing dye adsorption.

3.5. Adsorption isotherm

The adsorption isotherms give an equilibrium relationship between the amount of adsorbate adsorbed on the adsorbent's surface and its concentration in solution at

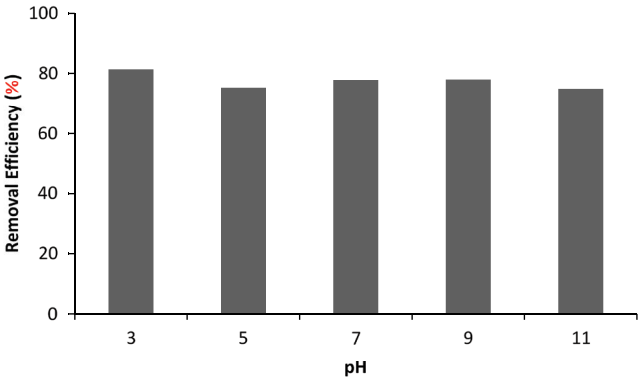

Fig. 9. The percentage removal of RR dye for different pH values of dye solutions (adsorption condition: room temperature; adsorbent dosage of 1 g/L; initial dye concentration of 30 ppm).

a constant temperature. Numerous adsorption models are available to fit the experimental adsorption data.

In this study, Langmuir and Freundlich isotherm models were chosen to fit the data. The linearised mathematical equations of the isotherm models were applied to fit the equilibrium data as they are convenient and more ordinarily used by previous researchers. The applicability of these isotherm models to fit the equilibrium data was compared by observing the correlation coefficient (R^2) values. The closer the R^2 value to 1, the better the fit. Besides, the SSE value closer to 0 indicates that these two models have a minor random error component and the fit will be more useful for prediction. Table 1 shows the Langmuir and Freundlich isotherm constants of RR dye adsorption onto the adsorbent.

Based on Table 1, the RH5%-DWTS shows relatively better linearity for the Freundlich isotherm model (R^2 = 0.973) compared to the Langmuir isotherm model (R^2 = 0.435). The R^2 value of the Freundlich model exceeds 0.9, suggesting that the model fits well with the experimental results. The adsorption of RR molecules onto RH5%-DWTS is multilayer adsorption. In multilayer adsorption, the adsorption space usually contains more than one

Table 1
Langmuir and Freundlich isotherm constants of RR dye adsorption onto RH5%-DWTS

Isotherm model	Adsorbent	RH5%-DWTS
Langmuir isotherm	Q_m (mg/g)	1,495.12
	b (L/mg)	371.17
	R^2	0.435
	SSE	0.00547
Freundlich isotherm	n	0.875
	K_f ((mg/g)(L/mg)$^{1/n}$)	3.395
	R^2	0.973
	SSE	0.117

layer of molecules and not all adsorbed molecules are in contact with the adsorbent surface layer. The maximum adsorption capacity (Q_m) and the Langmuir adsorption equilibrium constant (b) calculated from the Langmuir model are 1,495.12 mg/g and 371.17 L/mg, respectively. From Table 1, the $1/n$ value for the Freundlich isotherm is larger than 1 which indicates cooperative adsorption, where the adsorbed solute attracts the solute in bulk, whereas the $1/n < 1$ denotes an ideal Langmuir isotherm for the study. Fig. 10 shows the equilibrium adsorption of RR predicted by the Freundlich and Langmuir isotherm models, respectively. The finding is similar to a previous study reporting that coconut mesocarp used as an adsorbent for RR showed an adsorption capacity of 3.97 mg/g [42]. Different origins and modification methods of RH produce modified RH with different physicochemical structures. The integration of DWTS and RH seems to have the potential to enhance the performance of RH. Variety adsorption models need to be considered to study the suitable adsorption mechanism of modified RH.

The adsorption of brilliant green dye using RH ash fitted the Langmuir isotherm model [43]. Modified RH treated with HCl for the adsorption of Direct Orange-26 (DO-26), Direct Red-31 (DR-31), Direct Blue-67 (DB-67), and Ever-direct Orange-3GL (EDO-3) dyes fitted well to

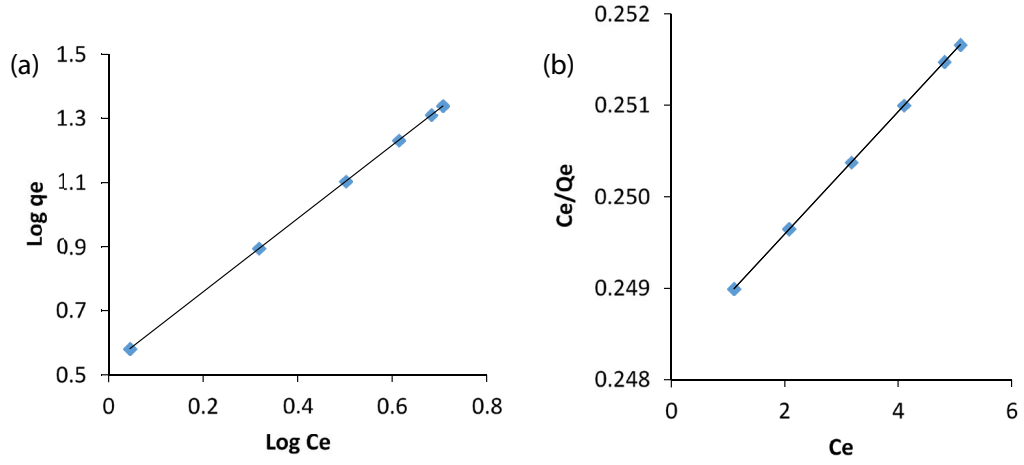

Fig. 10. Equilibrium adsorption of RR dye predicted by (a) Freundlich isotherm model and (b) Langmuir isotherm model.

the pseudo-second-order and Elovich kinetic models. Various functional groups attached to the biomass surface of hydroxyl, carboxylic, and amide groups have been identified using adsorption mechanisms [44]. Modified RH/magnetic alginate biocomposite demonstrated that the methylene blue (MB) adsorption fitted well to the nonlinear model described by the fractal Brouers-Sotolongo formalism with varied temperature [24]. The finding suggests the nature of the adsorption mechanism of anomalous diffusion to multi-site sorption of MB on biocomposite surfaces.

3.6. Analysis of variance

One-way ANOVA test was used in this study to validate the experimental data of the effect of adsorbent dosage, pH solution, and initial dye concentration. The ANOVA test was accomplished by determining the amount of dye adsorbed (mg/g) for each parameter. The null hypothesis denotes no significant difference between the data. If the observed F-value is higher than F_{crit} and the probability (p-value) is smaller than 0.05, then the null hypothesis is rejected. It means that the data has a significant difference between the means of groups. Table 2 shows the ANOVA of the amount of dye adsorbed for different adsorbent dosages. From the ANOVA comparison for different adsorbent dosages, it can be noticed that the F-value is larger than the F_{crit} and the p-value is less than 0.05, which means that the null hypothesis is rejected. Thus, there is a significant difference between the data for different adsorbent dosages for RR dye removal.

Table 3 presents the ANOVA of the amount of dye adsorbed at different pH for RR dye solutions. It shows that the amount of dye adsorbed increased with the decrease of the pH value of the adsorbate. The adsorption capacity is higher at a lower pH value. The ANOVA test shows that the F-value is higher than the F_{crit} and the p-value is higher than 0.05, indicating that the null hypothesis is rejected. Hence, there is a significant difference between the data for different pH values of dye solutions.

From Table 4, the amount of dye adsorbed increased with an increase in the initial dye concentration. The ANOVA of the amount of dye adsorbed for different initial dye concentrations obtained an F-value smaller than the F_{crit}, suggesting that the null hypothesis is accepted. This result indicates that there is no substantial variation between the data for different initial dye concentrations.

4. Conclusions

A modified adsorbent by combining RH and DWTS has a promising future as a low-cost adsorbent to remove RR dye. The R^2 values demonstrated satisfactory agreement

Table 2
ANOVA of the amount of dye adsorbed for different adsorbent dosages

Amount of dosage (g/L)	Amount of dye adsorbed (mg/g)	F-value	p-value	F_{crit}
1.0	21.847	854.0233	1.06E-07	5.987378
2.0	21.504			
3.0	21.417			
4.0	21.504			

Table 3
ANOVA of the amount of dye adsorbed for different pH values of dye solutions

pH value	Amount of dye adsorbed (mg/g)	F-value	p-value	F_{crit}
3	21.704	104.0004	7.33E-06	5.317655
5	21.544			
7	21.712			
9	21.744			
11	20.882			

Table 4
ANOVA of the amount of dye adsorbed for different initial dye concentrations of dye solutions

Initial dye concentration (mg/L)	Amount of dye adsorbed (mg/g)	F-value	p-value	F_{crit}
5	3.892	0.53705	0.480483	4.964603
10	7.919			
15	11.667			
20	15.750			
25	19.729			
30	24.410			

and fitted the Freundlich adsorption isotherm model. This model reveals multilayer adsorption for the adsorption of RR molecules on the adsorbent, which means that the adsorption space accommodates more than one layer of molecules. Based on the ANOVA study, the adsorbent dosage affects the efficiency of the adsorbent in removing RR dye. Therefore, the modified adsorbent is a promising adsorbent for dye removal in wastewater treatment due to the abundance of native adsorbent (RH) and good performance in dye removal.

Acknowledgement

The authors wish to thank the Centre of Research and Innovation Management (CRIM), Universiti Malaysia Terengganu for funding this research (Vot 53243) and Faculty of Ocean Engineering, Technology, and Informatics, Universiti Malaysia Terengganu for the contribution and support.

References

[1] M.Y.A. Razak, Compendium of Environment Statistics Malaysia 2020, Department of Statistics, Malaysia, 2020 (Retrieved on 23 December 2020). Available at: https://www.dosm.gov.my/v1/index.php?r=column/cthemeByCat&cat=162&bul_id=TjM1ZlFxb3VOakdmMnozVms5dUlKZz09&menu_id=NWVEZGhEVlNMeitaMHNzK2htRU05dz09

[2] N.H. Adenan, Y.Y. Lim, A.S.Y. Ting, Discovering decolorization potential of triphenylmethane dyes by actinobacteria from soil, Water Air Soil Pollut., 231 (2020) 560 (1–13), doi: 10.1007/s11270-020-04928-w.

[3] L. Ramakreshnan, A. Rajandra, N. Aghamohammadi, C.S. Fong, S. Nalatambi, A preliminary insight into the environmental awareness of community in the vicinity of batik manufacturing units in Kelantan, Malaysia, GeoJournal, 85 (2020) 1745–1753.

[4] S. Moosavi, C.W. Lai, S. Gan, G. Zamiri, O. Akbarzadeh Pivehzhani, M.R. Johan, Application of efficient magnetic particles and activated carbon for dye removal from wastewater, ACS Omega, 5 (2020) 20684–20697.

[5] M. Manogaran, B. Manogaran, A.R. Othman, B. Gunasekaran, M.Y. Abd Shukor, Decolourisation of Reactive Red 120 by a heavy metal-tolerant bacterium isolated from Juru River, Malaysia, Biorem. Sci. Technol. Res., 8 (2020) 23–26.

[6] F. Mcyotto, Q. Wei, D.K. Macharia, M. Huang, C. Shen, C.W.K. Chow, Effect of dye structure on color removal efficiency by coagulation, Chem. Eng. J., 405 (2021) 126674, doi: 10.1016/j.cej.2020.126674.

[7] M. Thanavel, P.O. Bankole, R. Selvam, S.P. Govindwar, S.K. Sadasivam, Synergistic effect of biological and advanced oxidation process treatment in the biodegradation of Remazol yellow RR dye, Sci. Rep., 10 (2020) 20234 (1–9), doi: 10.1038/s41598-020-77376-5.

[8] S. Varjani, P. Rakholiya, H.Y. Ng, S. You, J.A. Teixeira, Microbial degradation of dyes: an overview, Bioresour. Technol., 314 (2020) 123728, doi: 10.1016/j.biortech.2020.123728.

[9] M.Y. Chong, Y.J. Tam, Bioremediation of dyes using coconut parts via adsorption: a review, SN Appl. Sci., 2 (2020) 187 (1–16), doi: 10.1007/s42452-020-1978-y.

[10] J.H. Franco, B.F. da Silva, E.F.G. Dias, A.A. de Castro, T.C. Ramalho, M.V.B. Zanoni, Influence of auxochrome group in disperse dyes bearing azo groups as chromophore center in the biotransformation and molecular docking prediction by reductase enzyme: implications and assessment for environmental toxicity of xenobiotics, Ecotoxicol. Environ. Saf., 160 (2018) 114–126.

[11] N. Saksono, D.A. Putri, D.R. Suminar, N. Saksono, D.A. Putri, D.R. Suminar, Degradation of Remazol Red in Batik Dye Waste Water by contact glow discharge electrolysis method using NaOH and NaCl electrolytes, Int. J. Sci. Res. Knowledge, 1823 (2017) 020004 (1–7), doi: 10.1063/1.4978077.

[12] M.S.H. Bhuiyan, M.Y. Miah, S.C. Paul, T.D. Aka, O. Saha, M.M. Rahaman, M.J.I. Sharif, O. Habiba, M. Ashaduzzaman, Green synthesis of iron oxide nanoparticle using *Carica papaya* leaf extract: application for photocatalytic degradation of remazol yellow RR dye and antibacterial activity, Heliyon, 6 (2020) e04603, doi: 10.1016/j.heliyon.2020.e04603.

[13] T. Robinson, G. McMullan, R. Marchant, P. Nigam, Remediation of dyes in textile effluent: a critical review on current treatment technologies with a proposed alternative, Bioresour. Technol., 77 (2001) 247–255.

[14] M.A. Kamaruddin, M.S. Yusoff, H.A. Aziz, C.O. Akinbile, Recent developments of textile waste water treatment by adsorption process: a review, Int. J. Sci. Res. Knowledge, 1 (2013) 60–73, doi: 10.12983/ijsrk-2013-p060-073.

[15] B.M. D'Antoni, F. Iracà, M. Romero, Current treatment technologies and practical approaches on textile wastewater dyes removal, Panta Rei Srl – Water Solutions, (2017) 1–10, doi: 10.13140/RG.2.2.11472.71689.

[16] M.T. Yagub, T.K. Sen, S. Afroze, H.M. Ang, Dye and its removal from aqueous solution by adsorption: a review, Adv. Colloid Interface Sci., 157 (2019) 248–252.

[17] M.S. Santhosh, G. Karthikeyan, R. Sasikumar, R. Hariharan, R. Mohanraj, Mechanical and morphological behaviour of rice husk/prosopis juliflora reinforced bio composites, Mater. Today: Proc., 27 (2020) 556–560.

[18] M. Akhtar, M.I. Bhanger, S. Iqbal, S.M. Hasany, Sorption potential of rice husk for the removal of 2,4-dichlorophenol from aqueous solutions: kinetic and thermodynamic investigations, J. Hazard Mater., 128 (2006) 44–52.

[19] M. Shaban, M.R. Abukhadra, A.S. Mohamed, M.G. Shahien, S.S. Ibrahim, Synthesis of mesoporous graphite functionalized by nitrogen for efficient removal of safranin dye utilizing rice husk ash; equilibrium studies and response surface optimization, J. Inorg. Organomet. Polym. Mater., 28 (2018) 279–294.

[20] E.C. Peres, N. Favarin, J. Slaviero, A.R.F. Almeida, M.P. Enders, E.I. Muller, G.L. Dotto, Bio-nanosilica obtained from rice husk using ultrasound and its potential for dye removal, Mater. Lett., 231 (2018) 72–75.

[21] A.M. Akbar Ali, R.K. Karthikeyan, M. Sentamil Selvan, K.R. Mithilesh, M. Priyadharshini, N. Maheswari, G. Janani Sree, V.C. Padmanaban, R.S. Singh, Removal of Reactive Orange 16 by adsorption onto activated carbon prepared from rice husk ash: statistical modelling and adsorption kinetics, Sep. Sci. Technol., 55 (2020) 26–34.

[22] M.P. da Rosa, A.V. Igansi, S.F. Lütke, T.R. Sant'Anna Cadaval Jr., A.C.R. do Santos, A.P. de Oliveira Lopes Inacio, L.A. de Almeida Pinto, P.H. Beck, A new approach to convert rice husk waste in a quick and efficient adsorbent to remove cationic dye from water, J. Environ. Chem. Eng., 7 (2019) 103504, doi: 10.1016/j.jece.2019.103504.

[23] Z. Jiang, D. Hu, Molecular mechanism of anionic dyes adsorption on cationized rice husk cellulose from agricultural wastes, J. Mol. Liq., 276 (2019) 105–114.

[24] E. Alver, A.Ü. Metin, F. Brouers, Methylene blue adsorption on magnetic alginate/rice husk bio-composite, Int. J. Biol. Macromol., 154 (2020) 104–113.

[25] S. Sohrabnezhad, S.D. Mooshangaie, In situ fabrication of n-type Ag/AgBr nanoparticles in MCM-41 with rice husk (RH/MCM-41) composite for the removal of Eriochrome Black-T, Mater. Sci. Eng. B, 240 (2019) 16–22.

[26] T. Ahmad, K. Ahmad, M. Alam, Sustainable management of water treatment sludge through 3'R' concept, J. Cleaner Prod., 124 (2016) 1–13.

[27] Z. Meng, Z. Zhou, D. Zheng, L. Liu, J. Dong, Y. Yang, X. Li, T. Zhang, Optimizing dewaterability of drinking water treatment sludge by ultrasound treatment: correlations to sludge physicochemical properties, Ultrason. Sonochem., 45 (2018) 95–105.

[28] S. Hamzah, N.A. Ali, A.W. Mohammad, M.M. Ariffin, A. Ali, Design of chitosan/PSF self-assembly membrane to mitigate

fouling and enhance performance in trypsin separation, J. Chem. Technol. Biotechnol., 87 (2012) 1157–1166.
[29] S.H. Tang, M.A.A. Zaini, Malachite green adsorption by potassium salts-activated carbons derived from textile sludge: equilibrium, kinetics and thermodynamics studies, Asia-Pac. J. Chem. Eng., 12 (2016) 159–172.
[30] J.M. Salman, B.H. Hameed, Adsorption of 2,4-dichlorophenoxyacetic acid and carbofuran pesticides onto granular activated carbon, Desalination, 256 (2010) 129–135.
[31] P.A.M. Mourao, P.J.M. Carrott, M.M.L. Ribeiro Carrott, Application of different equations to adsorption isotherms of phenolic compounds on activated carbons prepared from cork, Carbon, 44 (2006) 2422–2429.
[32] L. Anah, N. Astrini, Isotherm adsorption studies of Ni(II) ion removal from aqueous solutions by modified carboxymethyl cellulose hydrogel, IOP Conf. Ser.: Earth Environ. Sci, 160 (2018) 012017.
[33] E. Liu, G. Kashwani, L. Li, Transformation of industrial solid wastes into carbon-infused infrastructure materials, J. Cleaner Prod., 260 (2020) 120890, doi: 10.1016/j.jclepro.2020.120890.
[34] N.A.M. Bashar, Z.H. Zubir, A. Ayob, S. Alias, Water treatment sludge as an alternative liner for landfill site: FTIR and XRD analysis, AIP Conf. Proc., 1774 (2016) 030026, doi: 10.1063/1.4965082.
[35] N.H. Shalaby, E.M.M. Ewais, R.M. Elsaadany, A. Ahmed, Rice husk templated water treatment sludge as low-cost dye and metal adsorbent, Egypt. J. Pet., 26 (2017) 661–668.
[36] I. Tan, L. Lim, K. Lim, Removal of atrazine from aqueous solutions using HNO_3 treated oil palm shell-based adsorbent, J. Civ. Eng. Sci. Technol., 4 (2013) 17–22.
[37] X. Xu, X. Cao, L. Zhao, Comparison of rice husk- and dairy manure-derived biochars for simultaneously removing heavy metals from aqueous solutions: role of mineral components in biochars, Chemosphere, 92 (2013) 955–961.
[38] J.N. Nsami, J.K. Mbadcam, The adsorption efficiency of chemically prepared activated carbon from cola nut shells by $ZnCl_2$ on methylene blue, J. Chem., 2013 (2013) 469170 (1–7), doi: 10.1155/2013/469170.
[39] T.R. Waghmode, M.B. Kurade, A.N. Kabra, S.P. Govindwar, Degradation of Remazol Red dye by *Galactomyces geotrichum* MTCC 1360 leading to increased iron uptake in *Sorghum vulgare* and *Phaseolus mungo* from soil, Biotechnol. Bioprocess Eng., 17 (2012) 117–126.
[40] M.M. Ibrahim, Cr_2O_3/Al_2O_3 as adsorbent: physicochemical properties and adsorption behaviors towards removal of Congo red dye from water, J. Environ. Chem. Eng., 7 (2019) 102848, doi: 10.1016/j.jece.2018.102848.
[41] M.A.A. Zaini, Y. Amano, M. Machida, Adsorption of heavy metals onto activated carbons derived from polyacrylonitrile fiber, J. Hazard. Mater., 180 (2010) 552–560.
[42] M.S. Monteiro, R.F. de Farias, J.A.P. Chaves, S.A. Santana, H.A.S. Silva, C.W. Bezerra, Wood (*Bagassa guianensis Aubl*) and green coconut mesocarp (*cocos nucifera*) residues as textile dye removers (Remazol Red and Remazol Brilliant Violet), J. Environ. Manage., 204 (2017) 23–30.
[43] V.S. Mane, I.D. Mall, V.C. Srivastava, Kinetic and equilibrium isotherm studies for the adsorptive removal of Brilliant Green dye from aqueous solution by rice husk ash, J. Environ. Manage., 84 (2007) 390–400.
[44] H.N. Bhatti, Y. Safa, S.M. Yakout, O.H. Shair, M. Iqbal, A. Nazir, Efficient removal of dyes using carboxymethyl cellulose/alginate/polyvinyl alcohol/rice husk composite: adsorption/desorption, kinetics and recycling studies, Int. J. Biol. Macromol., 150 (2020) 861–870.